# Design and Control of an Innovative Electronic Load for the Photovoltaic Module Characterization

CARUSO Massimo[1], DI NOIA Luigi Pio [2], FRICANO Michele[1], PIRRONE Giuseppe[1], SPATARO Ciro[1], VIOLA Fabio[1]

[1]University of Palermo, Italy
DEIM-Palermo, Italy;
Viale delle Scienze, Ed. 9, 90128 Palermo (PA), Italy, ciro.spataro@unipa.it

[2]University of Naples Federico II, Italy
DIETI- Napoli, Italy;
Via Claudio 21, 80125 Napoli (NA), Italy, luigipio.dinoia@unina.it

***Abstract*** **– *The paper proposes a new electronic load setup for a fast, low-cost and standard-compliant characterization of a photovoltaic module. The approach is based on the use of a DC–DC converter, exploiting its ability to emulate a resistor. In particular, a Buck-Boost converter topology is employed. The model is implemented in the Simulink/SimPower System environment. A commercial PV Conergy E215P photovoltaic module is used in order to evaluate the performances of the proposed electronic load and to validate the proposed approach.***

***Keywords:*** ***PV module; DC–DC converter; electronic load; PV characterization.***

## I. INTRODUCTION

In order to reduce the electrical energy production impact on the environment, society is paying more and more attention to renewable energy sources [1]. The transition from traditional fossil fuel plants to renewable ones can be obtained only by developing such technologies [2-6], and utilize them in smart grids within the distributed generation concept and considering in some cases co-generation systems [7-10], the power flow and energy management can be optimized thanks to the advances in power electronic apparatuses technology [11-15]. The photovoltaic is one of the most promising, both in short and long terms. This circumstance is highlighted by the rapid growth of the total photovoltaic (PV) power installed worldwide, which nowadays is higher than 100 $GW_p$.

For this reason, the researchers are focusing their efforts on the efficiency improvement of the PV technologies [16,17]. To perform this task, one of the main challenge is carrying out a correct characterization of the PV modules, taking into account that the method utilized for the PV module characterization must be able to give the results in a time lower than the time in which the weather conditions may change. In particular the most important parameters of a PV module is the *I-V* curve which is obtained with the use of a variable load, in accordance with the international standard [18]. The most effective type of load which is possible to use for the quickly characterization of PV module is the electronic load [19]. The aim of this paper is to propose the use of a buck-boost converter for the acquisition of the PV module parameters.

The main idea is to control the DC-DC converter to emulate a time-variant non-linear load for the PV module. The classical Buck and Boost converters are not capable to reproduce the whole *I–V* curve of PV generators, instead the Buck-Boost topology is optimal for this application [20,21].

For the Buck topology, the input resistance $R_{in}$ in Continuous Conduction Mode (*CCM*) must have a value in the interval $R_{in}$ (*CCM*) $\in [R_L, \infty)$. Therefore, according to this expression, a Buck converter cannot emulate smaller impedances than the load impedance, and therefore, it does not reach values near the short-circuit current of the PV module when it is used to obtain a *I–V* curve. For the Boost topology, the input resistance $R_{in}$ (*CCM*) must have a value in the range [0, $R_L$]. This expression indicates that a Boost converter cannot emulate impedances greater than the impedance of the load and, therefore, it does not reach values near the open circuit voltage of the PV module. For Buck-Boost topology $R_{in}$ (*CCM*) $\in [R_L, \infty)$, therefore, these last configurations are capable to detect the whole *I–V* curve of a PV module in *CCM* from open-circuit voltage ($V_{oc}$) to short-circuit current ($I_{sc}$) condition.

Accurate load modeling is the key of a successful conclusion of the overall design process. MATLAB/Simulink environment is best suited for data post processing and system simulation due to several co-simulation toolboxes, which allow simulating several heterogeneous models in a unique simulation environment.

In following section are reported the operation and the criteria design of the electronic load and the results of performed numerical simulations.

## II. ELECTRONIC LOAD FRAME

It is widely known that DC–DC converters increase or decrease the magnitude of the dc-voltage and/or invert its polarity. The electronic load here conceived is based on a DC-DC Buck-Boost converter, whose basic electrical circuit is shown in Fig. 1, in which diode D and switch SW are supposed to be ideal and $R_L$ is the resistive load.

The variation of the load current $i_{out}$ implies also the variation of the average inductor current, so the converter can operate in three ways:

1. Continuous Conduction Mode (*CCM*), in which the inductor current is continuous;
2. Discontinuous Conduction Mode (*DCM*), in which the inductor current is discontinuous;
3. Borderline Conduction mode (*BDC*) is the boundary between the continuous and discontinuous conduction mode.

For this application, the DC-DC converter is forced to a Continuous Conduction Mode (*CCM*) of operation to reduce conduction losses.

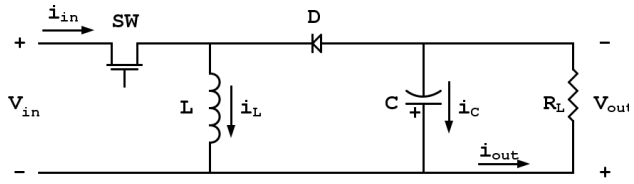


Fig. 1. Buck-Boost converter electrical circuit

For the CCM circuit shown in figure 1, the output voltage average value $V_{out,avg}$ can be expressed as a function of the input voltage $V_{in}$ and the duty cycle $\delta$, (being $\delta$ the ratio between the time $t_{on}$ in which SW is closed and the commutation time $T = t_{on} + t_{off}$ , where $t_{off}$ is the time in which the SW is open):

$$V_{out.avg} = \frac{\delta}{1-\delta} V_{in} \tag{1}$$

According to (1), by setting the $\delta$ value in the range [0, 1] and keeping the commutation time $T$ constant, it is possible to obtain the desired value of $V_{out,avg}$. Thus, the latter can be regulated by varying $\delta$. This technique is well known as PWM (Pulse Width Modulation) [22].

The *CCM* buck-boost topology here chosen has the following properties:

- the output voltage can be either greater or lower than the input voltage;
- as in the other topologies, if the joule losses are neglected, the conversion ratio $M$ appears to be independent from the load current. By varying the duty cycle $\delta$, it is possible to control the output voltage;
- there is a pulsating input ripple and a pulsating output current;
- as for the Buck, the power switch "floats", meaning that its control is more difficult.

Different techniques that simplify the converter studies have been proposed in literature. In 1986 Dr. Vorpérian developed the concept of the pulse width modulation (PWM) switch model [23], [24]. As the diode and the power switch introduced the nonlinearity, this researcher considered modeling the switch network alone, to finally replace it with an equivalent small-signal three-terminal model (nodes S, L, and D), in the same way of the transfer function of a bipolar amplifier.

By applying this theory to the converter, the equivalent circuital model shown in Fig. 2 is obtained. By applying the Kirchhoff Law at this model and by neglecting the parasitic element, the input resistance of the converter as a function of the duty cycle is:

$$R_{in} = \frac{R_L (1-\delta)^2}{\delta^2} \tag{2}$$

As shown by fig. 3, it is possible to use the buck-boost converter as electronic load, because, by acting on $\delta$, it is possible to vary the input resistance of the converter that represents the output equivalent resistance of the PV module.

In Fig. 4, a typical *I-V* characteristic curve of a generic PV module and several load lines corresponding to various $R_{in}$ values are plotted. The intersection between the load characteristic, which is related to a given duty cycle value, and the PV module *I-V* characteristic curve is a working point ($V_x$, $I_x$).

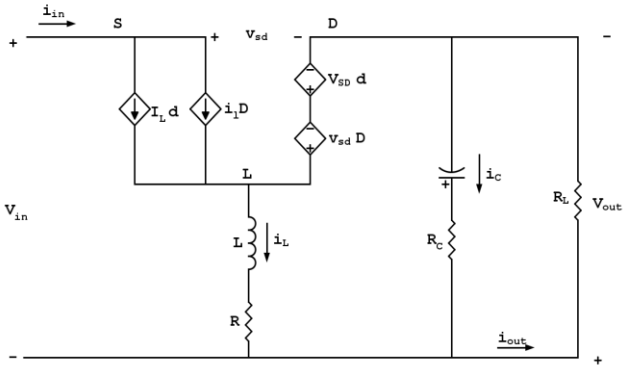


Fig. 2. Circuital model of the converter

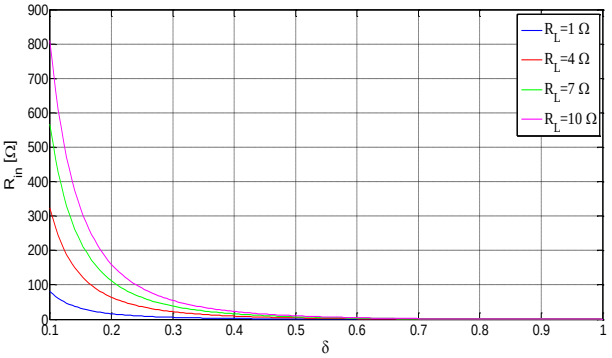


Fig. 3. Input resistance Vs Duty cycle (CCM)

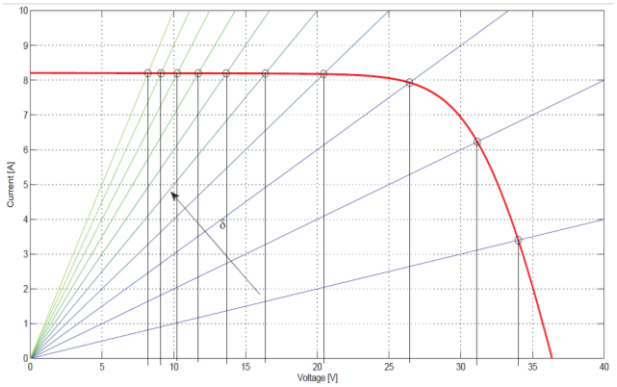


Fig. 4. Some static operation points

## III. ELECTRONIC LOAD CRITERIA DESIGN

The electronic load designed was validated on a 250 *W* commercial module Conergy E215P. Starting from the electric specifications of this PV module, the following design data for the electronic load have to be taken into account:

*TABLE 1 Designed data of electronic load*

| $V_{in,\,min}$ [V] | $V_{in,\,max}$ [V] | $I_{in,\,min}$ [A] | $I_{in,\,max}$ [V] | $P_n$ [W] |
|---|---|---|---|---|
| 0 | 40 | 0 | 10 | 250 |

The duty-cycle range is selected within 0.1 and 0.9, in order to acquire the points of the *I-V* curve from short circuit to open circuit. The chosen switching frequency is equal to 100 *kHz*, so the switching period $T_{SW}$ is 10 $\mu s$. This value of switching frequency has been chosen in order to minimize both the size of the filter components *L* and *C* shown in Fig.1 and the total conduction losses [25].

The $R_L$ load resistant value must be small enough to enable the determination of the characteristic points close to the short circuit one. This resistance must be also able to dissipate the electric power generated by the PV module under test, giving, at the same time, high accuracy. From the *I-V* simulated characteristic of the module under the standard conditions, it is possible to derive the maximum value of the input resistance, which is obtained when the voltage takes the maximum value $V_{in,max,CCM}$ and the current takes the minimum value $I_{in,min,CCM}$ assumed equal to 0.1 *A*. The value of this resistance is:

$$R_{in,\max.CCM} = \frac{V_{in,\max.CCM}}{I_{in,\max.CCM}} = \frac{36{,}326}{0{,}1} = 363.26\ \Omega \quad (3)$$

This value corresponds to the minimum value of the duty cycle $\delta_{min}$= 0.1. Therefore, from (2) the following expression is obtained:

$$R_L \le \frac{\delta_{\min}^2 \cdot R_{in,\max.CCM}}{(1-\delta)^2} = \frac{0{,}1^2 \cdot 363.26}{(1-0{,}1)^2} = 4{,}48\ \Omega \quad (4)$$

The buck-boost converter works in CCM mode of operation, if (5) is ensured under each operating condition, in which the most critical condition corresponds to $\delta = \delta_{min} = 0.1$:

$$L \ge \frac{V_{in,\max.CCM} \cdot T_{SW} \cdot \delta}{2 \cdot I_{in,\max.CCM}} = 16{,}38\mu\text{H} \quad (5)$$

Eq.5 allows obtaining the minimum value of the inductor to ensure the CCM operation.

The choice of the capacitor can be done by taking into consideration the output voltage ripple. In fact, by assuming that all the ripple current component of the output current flows through the capacitor and its average value flows through the load resistor, the peak-to-peak voltage ripple can be calculated as follows:

$$\frac{\Delta V_{out}}{V_{out}} = \frac{\delta_{\max} \cdot T_{SW}}{R_L \cdot C} \quad (6)$$

Therefore:

$$C \ge \frac{\delta_{\max} \cdot T_{SW}}{R_L \cdot \left(\frac{\Delta V_{out}}{V_{out}}\right)} = 112\ \mu\text{F} \quad (7)$$

where $\delta_{max}$ = 0.9 and $\Delta V_{out}/V_{out} \le 2\%$ because in this case no special requirements on the output voltage ripple are needed.

The AC inductor current ripple flows along the series of *C* and a resistor $R_C$ (the equivalent inductor is neglected). Depending on the value assumed by $R_C$, the output voltage ripple can be significantly affected [26].

The drop voltage occurring in this element is given by:

$$\Delta V_{R_c} = \Delta I_C \cdot R_C \quad (8)$$

Eq.8 allows obtaining the maximum $R_C$ value, according to the following equation:

$$R_C \le \left\{ \left(\frac{\Delta V_{out}}{V_{out}}\right) \cdot \left[ \frac{1}{R_L \cdot (1-\delta)} + \frac{(1-\delta) \cdot T_{SW}}{2 \cdot L} \right]^{-1} \right\} \quad (9)$$

By varying the duty cycle, is possible to obtain the $R_C$-$\delta$ trend shown in Fig. 5. The maximum value of $R_C$ is:

$$R_C \le 36{,}2\ m\Omega \quad (10)$$

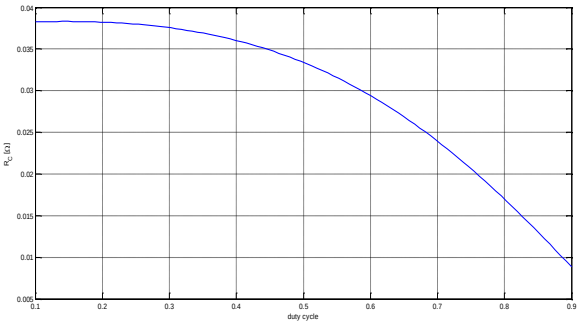


Fig. 5. Trend of $R_C$ as function of the duty cycle

Since the switching frequency is relatively high, it is possible to use a Schottky diode that allows a low forward voltage drop and a very fast switching action.

The design constraints, like the voltage and the switching frequency, require choosing the N-channel power mosfet for this application. Input voltage levels prohibit the use of direct-gate drive circuits for high-side N-channel power mosfet. Consequently, the principle of bootstrap gate-drive technique is used [27].Table 2 summarizes the converter parameters.

*TABLE* 2. *Value of designed buck-boost.*

| Component | Productor code | Main Characteristics |
|---|---|---|
| Mosfet | IRF B4410ZPBF | 97 A – 100 V |
| Driver mosfet | FAN73711 | ---------- |
| Inductor | PVC 033312L | 33 µH – 11 A |
| Diode | STP S10SM80CR | 11 A – 80 V |
| Capacitor | EEUFC1H121 | 120 µF – 50 V |
| Load resistance | THS 503R9J | 3.9 Ω - 50 W |

The electronic load was designed by using the Simulink/SimPowerSystem software and the simulation results are described in the next section.

## IV. SIMULATION RESULTS

In order to simulate the behavior of the electronic load in Simulik/SimPowerSystem, a mathematical and circuital model of the PV module was implemented [28,29] in accordance with its datasheet.

The role of the control system in the DC-DC converters mainly consists in maintaining its stability properties in case of parametric variations.

The purpose of the electronic load is to vary the input resistance of the converter ($R_{in}$), which is the equivalent output resistance of PV module, from a maximum value to a minimum value. For the electronic load control a feedback system is used, in which the output signal is sampled and, then, fed back to the input in order to generate an error signal that drives the system [30].

Fig. 6 shows a schematic diagram of a DC-DC converter with the feedback system.

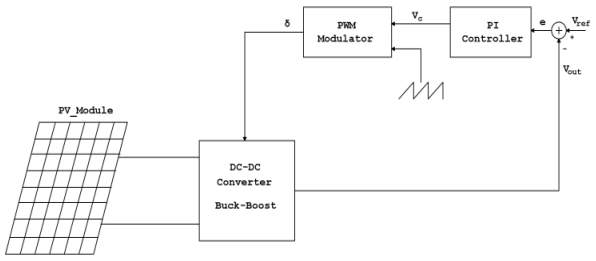


Fig. 6. Scheme of a DC-DC Converter with feedback system

Since the $R_{in}$ is function of $V_{out}$, it is possible to state that:

- $V_{out}$ accounts for the output signal;
- $V_{ref}$ accounts for the input signal;
- $V_c$ accounts for the control variable.

Therefore, the error signal is processed from a PI controller with anti-windup, which minimizes the error over time by adjustment of the control variable $V_c$. $V_c$ is, then, compared with the sawtooth signal and the modulator generates the PWM signal with a given duty cycle. A variation of $\delta$ corresponds to a variation of $R_{in}$.

In this case, $V_{ref}$ is defined in standard condition (1000 W/m$^2$ and 25 ℃). Therefore, the characterization of the PV module must be measured in a climatic environment.

The simulation results of the proposed system are shown in Fig. 7, Fig. 8 and Fig. 9. In order to simplify the simulation, only seven steps of voltage variation were considered.

Fig. 7 shows the overlapping patterns of the reference voltage (in blue) and the output voltage of the converter (in green). This circumstance validates the correct application of the control strategy.

Fig. 8 and Fig. 9 show the output voltage drop and the output current rise for each step of $R_{in}$ variation.

It is possible to notice that, after a transient of about 10 *ms*, both the output voltage and current stabilize at the reference value. Therefore, it is possible to acquire the *I-V* points of the curve in a very fast manner.

Fig. 10 reports an image of the experimental set up of the electronic load.

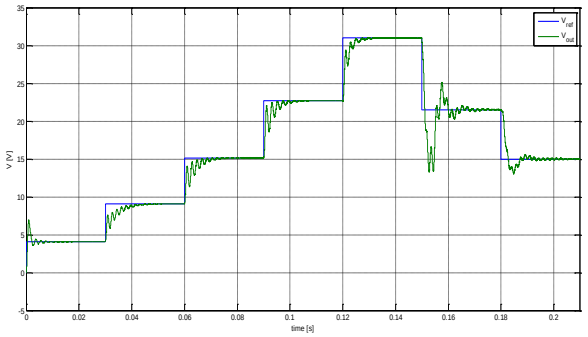

Fig. 7. Comparison between the output voltages of the converter and the reference voltage

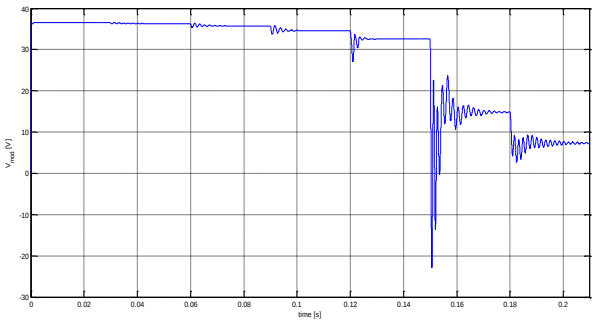

Fig. 8. Output voltage of the PV module

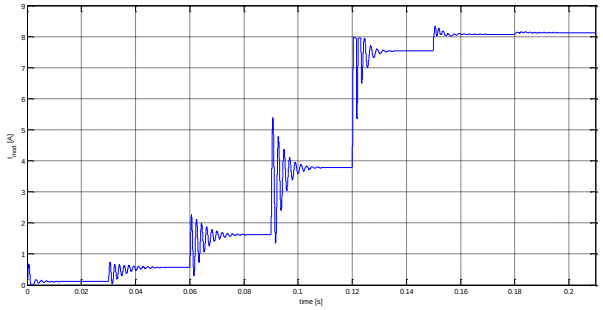

Fig. 9. Output current of the PV module

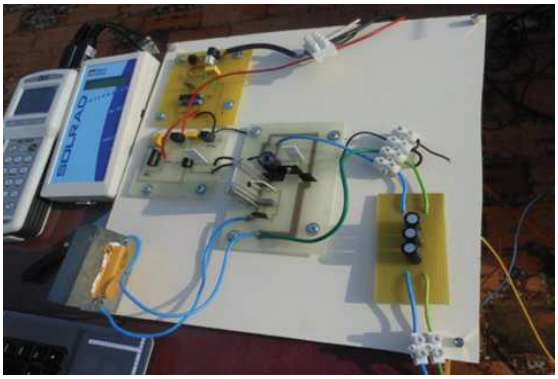

Fig. 10. Electronic load experimental set up

Fig. 11 shows the comparison of the simulation results under standard conditions when the voltage is increased. The points of the *I-V* curve, acquired by the proposed system, are plotted in red color, while the graph from the datasheet of the PV module is plotted in black. The same figure demonstrates the accordance between the two trends.

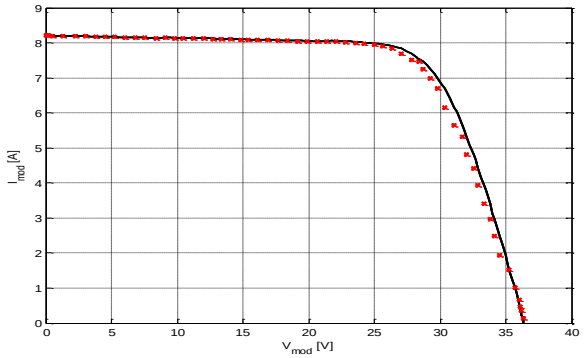

Fig. 11. *I –V* curve at 1000 W/m$^2$ and 25°C

On the market, there are different type of electronic load for the characterization of the PV modules. These loads have the same performances of the here proposed electronic load, but are more expensive and bulky. In Table 3, the specifications of the main electronic loads available on the market are compared with the specifications of the proposed electronic load. It can be observed that the proposed electronic load shows the best performances and allows a reliable, low-cost and fast measurement for the working conditions detection of the PV modules.

*TABLE3. Comparison of the main commercially available electronic loads.*

| Producer | Producer code | P [W] | $V_x$ [V] | $I_x$ [A] | WxHxD [mm] | Price € |
|---|---|---|---|---|---|---|
| B&K Precision | BK8600 | 150 | 120 | 30 | 214.5×88.2 ×354.6 | 1.250 |
| Keithley | 2380-500-15 | 200 | 500 | 15 | 482×131.4 ×580 | 1.820 |
| B&K Precision | BK8602 | 200 | 500 | 15 | 214.5×88.2 ×354.6 | 1.490 |
| B&K Precision | MDL200 | 200 | 80 | 40 | 82×183×573 | 1.106 |
| Keysight | 6063B-240-902 | 250 | 240 | 10 | 425.5×101.6 ×396 | 3.355 |
| DC-DC Converter | | 250 | 40 | 10 | 200×50×100 | 250 |

## V. CONCLUSIONS

In the paper has been proposed a design methodology of a system utilized to detect the current and voltage curves of PV module by means of a DC-DC buck-boost power converter.

Some numerical and experimental simulations have been carried out by means of Simulink ©; the input of simulations were obtained using the commercial PV module E215P [31]. The goals of performed simulations are the evaluation of performance of PV module in accordance with the international standards, the output results confirm the goodness of the proposed setup.

## ACKNOWLEDGMENT

The authors acknowledge the financial and technical support from SDESLAB (Sustainable Development and Energy Saving LABoratory) of the University of Palermo.

## REFERENCES

[1] S. Favuzza, G. Graditi, M. G. Ippolito, F. Massaro, R. Musca, E. R. Sanseverino, and G. Zizzo, "*Transition of a distribution system towards an active network. Part I: Preliminary design and scenario perspectives*," Proc. ICCEP 2011, pp. 9–14, Jun. 2011.

[2] L. Dusonchet, S. Favuzza, F. Massaro, and G. Morello, "*Economic financial analysis of investments in the photovoltaic sector in Italy*", Energia Elettrica, vol. 86, no. 3, pp. 37–51, 2009.

[3] A.O. Di Tommaso, F. Genduso, R. Miceli, "*Analytical investigation and control system set-up of medium scale PV plants for power flow management*", Energies, Vol. 5, Issue 11, November 2012, pages 4399-4416.

[4] V. Boscaino, R. Miceli, G. Capponi, g. Ricco Galluzzo, "*A review of fuel cell based hybrid power supply architectures and algorithms foe household appliances*", Intern Journal of Hydrogen Energy, Vol. 39, 3, Jan 2014.

[5] L. Piegari, R. Rizzo, P. Tricoli, "*High efficiency wind generators with variable speed dual-excited synchronous machines*", International Conference on Clean Electrical Power ICCEP '07, pp. 795-800, 2007.

[6] L. Piegari, R. Rizzo, *"A control technique for doubly fed induction generators to solve flicker problems in wind*

*power generation"*, PECon 2006 Intern Power and Energy Conference, pp. 19-23, Malaysia, Nov 2006.

[7] R. Rizzo, P. Tricoli, "*Power flow control strategy for electric vehicles with renewable energy sources*", Proc. PECon 2006 - First International Power and Energy Conference, Putrajaya (Malaysia), Nov 2006.

[8] P. Capaldi, A. Del Pizzo, L. Piegari, R. Rizzo, "*A low cost microcogeneration system for domestic and industrial applications*", IEEE International Conference on Industrial Technology, Tunisia, Dec. 2004.

[9] P. Capaldi, A. Del Pizzo, R. Rizzo, I. Spina, "*Torque-oscillations damping in micro-cogeneration units with high brake mean pressure engines and PM-brushless generators*", Energy Conference and Exhibition ENERGYCON 2012, pp. 121-126, Florence, 2012.

[10] A. Dannier, R. Rizzo, "*An overview of Power Electronic Transformer: Control strategies and topologies*", Proc. SPEEDAM 2012 - 21st International Symposium on Power Electronics, Electrical Drives, Automation and Motion, pp. 1552-1557, Sorrento (Italy), 2012.

[11] G. Brando, R. Rizzo, "*An optimized algorithm for torque oscillation reduction in DTC-Induction motor drives using 3-Level NPC inverter*", Proc. IEEE ISIE 2004, pp. 1215-1220, Ajaccio (France), 2004.

[12] G. Brando, A. Coccia, R. Rizzo, "*Control method of a braking chopper to reduce voltage unbalance in a 3-level chopper*", IEEE International Conference on Industrial Technology, pp. 975-978, Tunisia, Dec. 2004.

[13] L. Piegari, R. Rizzo, P. Tricoli, "*A Comparison between Line-Start Synchronous Machines and Induction Machines in Distributed Generation*", Przeglad Elektrotechniczny, 88 (5b/2012), pp. 187-193, 2012.

[14] R. Rizzo, P. Tricoli, I. Spina, "*An innovative reconfigurable integrated converter topology suitable for distributed generation*", Energies, 5 (9), pp. 3640-3654, 2012.

[15] G. Brando, A. Dannier, R. Rizzo, "*A sensorless control of H-bridge multilevel converter for maximum power point tracking in grid connected photovoltaic systems*", International Conference on Clean Electrical Power ICCEP '07, pp. 789-794, Capri (Italy), May 2007.

[16] A. Andreotti, A. Del Pizzo, R. Rizzo, P. Tricoli, "*An efficient architecture of a PV plant for ancillary service supplying*", Proc. SPEEDAM 2010 - International Symposium on Power Electronics, Electrical Drives, Automation and Motion, Pisa (Italy), 14-16 June 2010.

[17] G. Cipriani, V. Di Dio, L.P. Di Noia, F. Genduso, D. La Cascia, R. Miceli, R. Rizzo, "*A PV plant simulator for testing MPPT techniques, 4th International Conference on Clean Electrical Power: Renewable Energy Resources Impact*",Proc. ICCEP 2013, Alghero, 2013.

[18] I. Standard, "*60904-1, Photovoltaic Devices, Part 1: Measurement of PV Current–Voltage Characteristics*," Intern. Electrotechnical Commission, Geneva, 2006

[19] Y. Kuai and S. Yuvarajan, "*An electronic load for testing photovoltaic panels*," Journal of Power Sources, vol. 154, no. 1, pp. 308–313, 2006.

[20] G. Cipriani, G. Ciulla, V. Di Dio, D. La Cascia, and R. Miceli, "*A device for PV modules IV characteristic detection*," ICCEP 2013, pp. 24–30, 2013.

[21] E. D. Aranda, J. A. G. Galan, M. S. de Cardona, J. M. A. Marquez, "*Measuring the I-V curve of PV generators*," IEEE Industr. Electronics Magazine, vol. 3, pp. 4–14, 2009.

[22] N. Mohan, T. M. Undeland, and W. P. Robbins, *Elettronica Di Potenza: convertitori e applicazioni*. U. Hoepli, 2005.

[23] V. Vorperian, "*Simplified analysis of PWM converters using model of PWM switch. Continuous conduction mode*," IEEE Transactions on Aerospace and Electronic Systems, vol. 26, no. 3, pp. 490–496, May 1990.

[24] E. Van Dijk, J. Spruijt, D. M. O'sullivan, and J. B. Klaassens, "*PWM-switch modeling of DC-DC converters*," IEEE Trans on Power Electronics, vol. 10, no. 6, pp. 659–665, 1995.

[25] A. Pressman, *Switching power supply design*. McGraw-Hill, Inc., 1997.

[26] E. C.Basso and R. Dampled, *Switch-mode power supplies spice simulations and practical designs*. 2007.

[27] Fairchild, *Design and Application Guide of Bootstrap Circuit for High-Voltage Gate-Drive IC*. Fairchild Semiconductor Corporation, 2008.

[28] M. G. Villalva, J. R. Gazoli, and E. R. Filho, "*Modeling and circuit-based simulation of photovoltaic arrays*" Power Electronics Conference, 2009. COBEP '09. Brazilian, pp. 1244–1254, 2009.

[29] V. Boscaino, G. Cipriani, V. Di Dio, R. Miceli, and G. Capponi, "*A simple and accurate model of photovoltaic modules for power system design*," EVER 2014, 2014.

[30] A. Prodic, D. Maksimovic, and R. W. Erickson, "*Design and implementation of a digital PWM controller for a high-frequency switching DC-DC power converter*,", IECON, 2001.

[31] Conergy E215P PV Module Datasheet. www.conergy.de.